Vol 16 No 1, p 127-131

NUMERICAL SIMULATION OF INSPIRATORY AIRWAY IN THE NASAL CAVITY OF A BACTRIAN CAMEL (*Camelus bactrianus*)

Hongju Wang, Zhongtian Bai, Chengjuan Gao and Jianlin Wang
School of Life Science, Lanzhou University, Lanzhou, Gansu 730000, PR China

ABSTRACT

To investigate the flow patterns in nasal cavity of bactrian camel (*Camelus bactrianus*), an anatomically accurate finite volume model of its left nasal cavity from CT scans of a healthy adult nose was constructed. By numerically solving the steady-state Navier-Strokes and continuity equations, the flow distribution and the complete velocity field for inspiration throughout the nasal cavity under physiological flow rates of breathing was studied. During inspiration, the highest velocity occurred along the nasal floor. The pressure droplet between the nostril and pharynx was about 7 pascal at the inspiratory flow rate of 232 ml/s. It was could concluded that the anatomical complexity makes the air cleaned and conditioned sufficiently. This technique may help understanding the physiological functions of the noses in camels.

Key words: Computational fluid dynamics (CFD), CT scan, nasal airflow, numerical simulation

Bactrian camel (*Camelus bactrianus*), who lives in desert, possesses some characteristics to adapt the live conditions. Their upper airway is one of the important physiological structure that helps in adaptation to the environment. The nasal cavity plays an important role in conditioning of inhaled air to a specific range of temperature, humidity, olfaction and removal of suspended particles and droplets. In camels, the lowest respiratory water loss and the humidity less than 100% in expiratory air can be explained by the exhalation of air at far below the body temperature (Schmidt Neilsen *et al,* 1981). There are 3 portions of nasal cavity in camels, i.e. the rostral, middle and caudal partitions. Nasal vestibule is located at the rostral portion, nasal conchea are located at the middle portion and ethmoidal conchea are situated at caudal portion (Smut and Bezuidenhout, 1987).

Scholars have used many techniques to study the physiological functions of upper airways. Respiratory dynamics is one of the important subject to study the respiratory process and many scholars built models to compute the physical fields. A model of respiratory heat transfer in Kangaroo rat (*Dipodomys spectabilis*) to compute values of energy transfer, expired air temperature, rate of water loss and so on was prepared (Collins *et al,* 1971). Today, Computational Fluid Dynamics (CFD) methods are profoundly used in science to simulate natural process, including numerous biomedical applications. Especially, numerical simulation of airflow in human nasal cavity is well developed to optimise the detailed flow phenomena without clinical risk for the patients. Though there are some idealisations in the process of simulation, previous study on human (Keyhani *et al,* 1995) revealed that the numerical results are agreeable with *in vitro* experimental observations. This technique will help us understanding the physiology of respiration in camels.

Methods to simulate airflows in nasal cavity of human, the Sprague-Dawley Rat (Yang *et al,* 2007) and *Rhesus Monkey* (Kepler *et al,* 1998) are reported. Present study simulated the airflow in nasal cavity of a camel to detail the velocity field during respiration. This study may help clinical research on the diseases of nasal cavity and their intra nasal treatments.

Materials and Methods

Surface reconstruction

A three-dimensional (3-D) picture of left nasal cavity camel was generated from a computed tomography (CT) scan in an adult healthy bactrian camel using a SIEMENS/SENSATION 64-slice spiral CT scanner. The scan resolution was 512×512 pixels and the distance between the slices was 0.7 mm. The scan used is shown in Fig 1. The model geometry of left nasal cavity was reconstructed

SEND REPRINT REQUEST TO JIANLIN WANG email: jlwang@lzu.edu.cn

using the commercial software package: AMIRA® (Mercury Computer System, Berlin). Construction of this geometric model was first performed a segmentation step to isolate the desired region for surface model generation, and the threshold choosen was 0-100 as min-and max values, and the region of intranasal air was labeled. Then manual corrections were made for fine adjustment and the region of nasal sinuses were removed to idealise and simplify the model for further research. A tube was added, whose transverse plane was similar with the nostril, to help constructing the grids of inlet. Smoothing was applied to the resulting surface model in order to avoid rough and irregular edges disturbing the simulated airflow. AMIRA® software was then used to successively construct a triangular surface and an unstructured volumetric tetrahedral grid of the object. The original mesh, AMIRA normal mesh (A-NM), was composed of 1,362,722 triangular faces for the surface grid and 730,898 tetrahedral cells for the volumetric grid (Fig 2 and 3). The quality of the mesh was estimated by the triangle aspect ratio (<10) and tetra aspect ratio (<10).

Numerical simulations

Numerical simulations of inspiratory airflows were performed in the reconstructed model derived from the left nasal cavity of bactrian camel. The commercial computational fluid dynamics (CFD) programme FLUENT 6.3.26 (Fluent Inc., Lebanon) was applied to accomplish it. The simulation was based on the numerical solution of the Navier-Strokes and continuity equations. At normal physiological flow rates, incompressible flow conditions were assumed. The boundary conditions were set as follows: The wall was of no-slip, the velocity which was set at velocity inlet was constant and the pressure in the outlet was set as zero pascal. The nasal airflow can be considered quasi-steady on the basis of the Strouhal parameter (S=wL/n) based on the axial length, L, from the entrance. For quiet restful breathing in frequency of 7-14 breath/min, the Strouhal parameter was less than 0.3, indicating that the quasi-steady approximation was reasonable (Pedley *et al,* 1977).

The finite volume mesh was used to calculate the velocity field for the uniform velocity of 0.6 m/s, 1 m/s, 1.5 m/s and 3 m/s, corresponding to flow rate of 139.2 ml/s, 232 ml/s, 348 ml/s and 464 ml/s during inspiration. The corresponding values of Reynold number *Re* at the inlets are 492, 821, 1231 and 1642. All Raynold numbers are lower and a laminar model for the flow rates 139.2 ml/s, 232 ml/s, 348 ml/s and 464 ml/s were used to simulate the flow field. This did not simulate real breathing perfectly since the flow was induced at the larynx drawing the air from the nostrils which is affected by geometrical differences leading to variable flow rates. However, for this paper, the focus was to study the flow patterns within the nasal cavity of camel under a steady-solution for lower flow rates.

Results

As the main objective was to use the CFD technique in this numerical modeling work, hence all subsequent results demonstrate only simulated, not measured fields in the nasal cavity.

Streamline patterns

Streamline patterns in the finite volume model were determined by introducing neutrally point particles released from the external nares plane, and tracking the path of them based on the computed flow field. Fig 4 shows that the main stream of the airflow at flow rate of 232 ml/s in nasal cavity of bactrian camel passed ventrally through the passages and exited through the naso-pharyngeal meatus without entering the ethmoid recess while the conchea structures direct the flow in an rostro-caudal direction. In an inspiratory flow mass of 464 ml/s, the velocity is still lower than other parts in dorsal meatus, but more particles were tracked here, which revealed that larger volumetric flow travelled in the olfactory area. The fraction of volumetric flow reaching the olfactory region changes with flow rates of inspiratory flow. The streamlines show that the number of particles tracked in olfactory region increased slightly as the flow rates increased during inspiration.

Velocity Profiles

The velocity profiles for predicted inspiratory flow are integrated over 9 selected coronal sections to determine the flow distribution throughout the nasal cavity of bactrian camel.

Iso-velocity contours plots determined from the numerical simulations for inspiratory flow rate of 232 ml/s are shown in Fig 5. As shown in Fig 5, the highest velocity of airflow in nasal cavity of bactrian camel occurs along the nasal floor and the secondary peak occurs at the middle meatus close to the nasal septum. The lowest airflow occurs through the superior region of the nasal cavity. The velocity decreases to nearly 0 ml/s at the caudal region of dorsal meatus where the particles released at the inlet couldn't be tracked and their trajectory misses.

Vector plots in Fig 6 show the secondary motion of flow at the inspiratory flow rate of 232 ml/s. The axial flow direction is perpendicular to the planes, whereas the secondary velocity vectors are in planes.

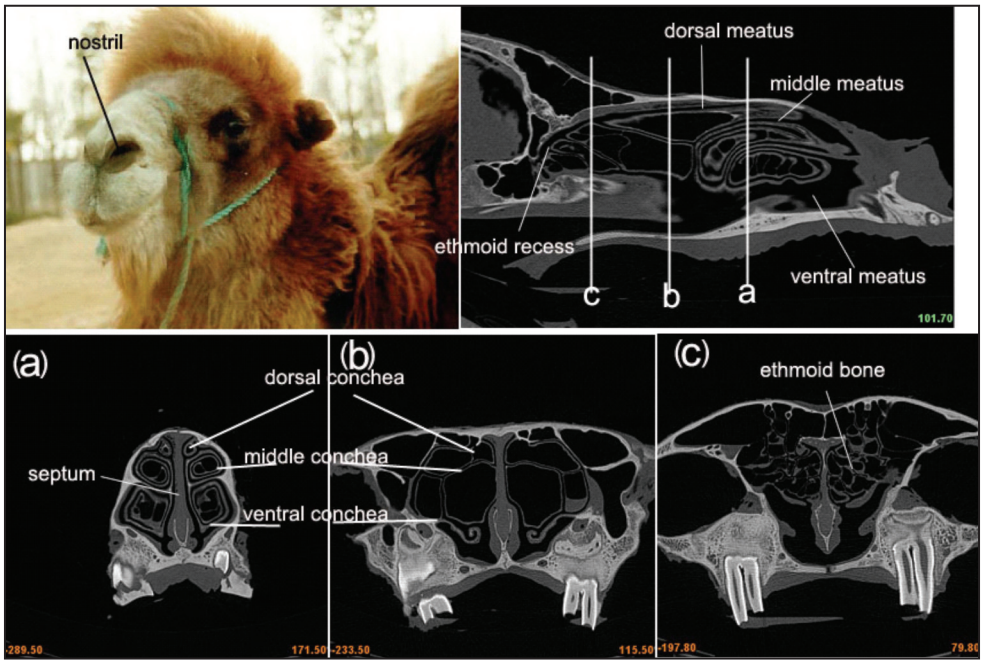

Fig 1. An image of a bactrian camel shows the position of its left nostril and four CT images (a), (b), (c) show three coronal sections corresponding lines a, b, c in a saggital section of nasal cavity.

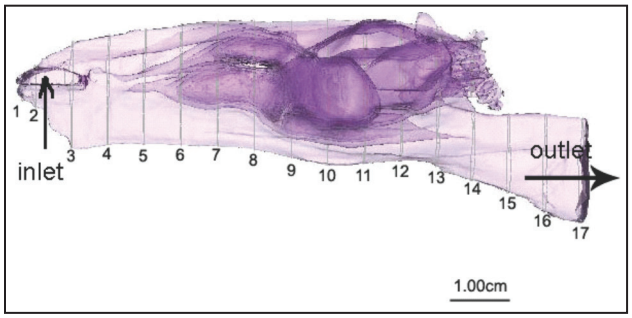

Fig 2. Lateral transparent view of the three-dimensional model of the left nasal passage in a bactrian camel.

The axial component of velocity is larger than the secondary component through most of the main nasal passages. As the airway changes, such as expansion and constriction, the secondary vectors of velocity become larger than that in unchangeable structures. The velocity profiles show negative-value axial flow in the rostral part of the nasal cavity because the airflow is obstructed and forced to change its direction (Fig 6). For example, on plane 1, the air flow is towards the rostral part at the side of the nasal septum, and turbulent flow appears in nasal vestibule.

Pressure drop and distribution of wall shear stress

According to the simulation results, the pressure drop increases as the flow rate increased. At the inspiratory flow rate of 232 ml/s, the drop of pressure between the nostril and pharynx is about 7 pascal. As the flow rates increase, the pressure drops also increase.

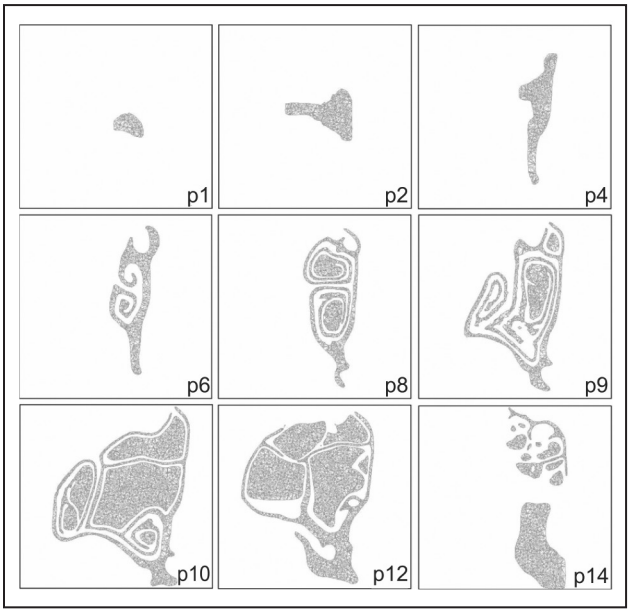

Fig 3. Nine selected cross sections of the finite volume mesh.

The wall shear stress distribution in planes in Fig 7 also shows a trend in accordance with the flow distribution. The maximum wall shear stress occurs near the narrow portion of the airway. As the conchea expands laterally and mostly occupies whole cavity, the main air passage narrows and the wall shear stress increases.

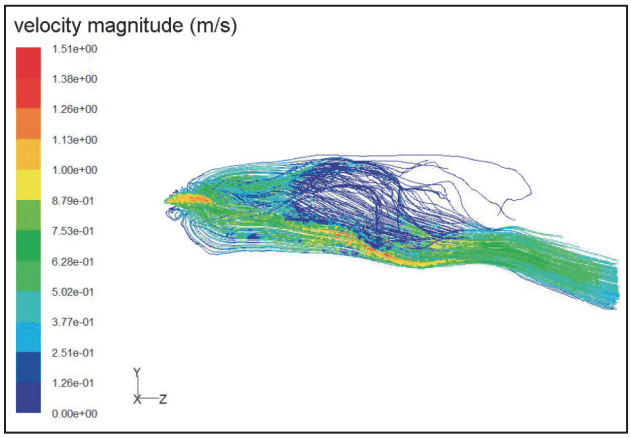

Fig 4. Pathline plots coloured by velocity magnitude in m/s at the inspiratory flow rate of 232 ml/s through the nasal model.

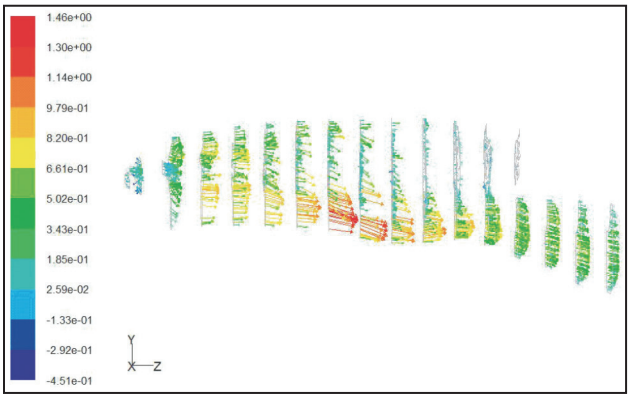

Fig 6. Velocity vector plots coloured by axial velocity (m/s) in 17 coronal planes at the inspiratory flow rate of 232 ml/s. Arrows show the movement directions of airflow.

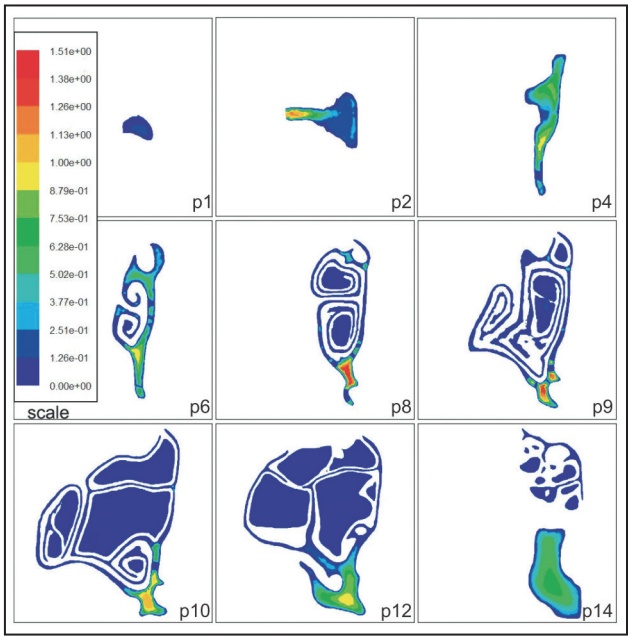

Fig 5. Contour plots of velocity magnitude during inspiration at flow rate of 232 ml/s in the 9 coronal planes. Top left corner: scale of velocity magnitude in m/s.

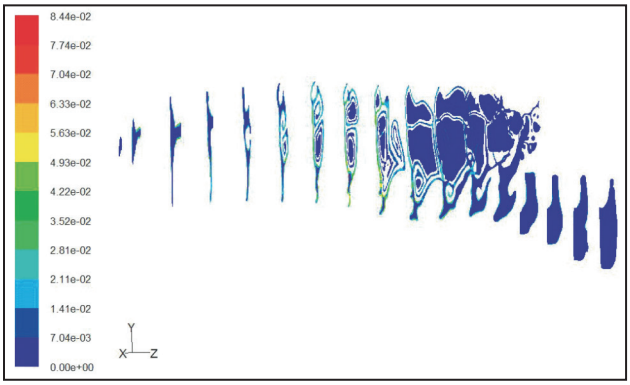

Fig 7. Plots of wall shear stress (Pascal) show its changes with structures of cavity.

Discussion

In our study, we tried to numerically simulate the laminar airflow in the nasal cavity of camels in terms of physiological phenomena. It's the first time to numerically simulate airways of the nasal cavity in camels.

It was demonstrated that the airways are very different with that in human, rats and Rhesus Monkey (Keyhani *et al,* 1995; Yang *et al,* 2007; Kepler *et al,* 1998). Because of the complex anatomical structures the nasal passage, resistance in camels is larger than other animals and the velocity decreases faster. But in our study we haven't measured the flow flux in different regions so we couldn't compare them to verify the conclusion.

Flow experiments in complex structures are difficult. Experimental verification of present results was not carried out. Present study is single model study; therefore, the results cannot be applied to different noses in bactrian camel. More simulations using other models with different shapes are needed to ascertain the flow characteristics in the camel's nasal cavity.

In present study, some simplifying assumptions were made. The airflow was approximated in nasal cavity of bactrian camel as being quasi-steady. This assumption has not been shown to be reasonable in nasal cavity of bactrian camel, but has been proved at quiet breathing rates in human. The nasal wall of camel was considered to be rigid hence during quiet breathing, the dimensions of the nasal cavity were nearly constant. Infact, mucous flow on the airway surface would also result in no-slip boundary conditions at the wall, but the presence of mucous on

the airway surface is expected to be negligible on the airflow velocity profiles. The flow rates were assumed to be uniform and the nostrils were opened all the time. These facts may simplify the calculations, but remained to be considered as parameters affecting the results.

This study, which used CFD softwares to analyse the flow patterns in nasal cavity of camels, will help us to physiological functions of camel's nose. The relative physiological functions of nasal cavity will change during the disease stress, e.g. dehydration, pyrexia etc.

References

Collins JC, Pilkington TC and Schmidt-Nielsen K (1971). A model of respiratory heat transfer in a Small Mammal. Biophysical Journal 11:886-914.

Kepler GM, Richardson RB, Morgan KT and Kimbell JS (1998). "Computer Simulation of Inspiratory Nasal Airflow and Inhaled Gas Uptake in a Rhesus Monkey." Toxicology and Applied Pharmacology 150(1):1-11.

Keyhani K, Scherer PW and Mozell MM (1995). Numerical simulation of airflow in the human nasal cavity. Journal of Biomechanical Engineering 117:429-441.

Pedley TJ, Schroter RC and Sudlow MF (1977). Gas flow and mixing in airways. In: Bioengineering Aspects of The Lung. Editor, West JB. New York: Marcel Dekker, Inc. pp 163-265.

Schimidt Nielsen EC Crawford and Hammel HT (1981). Respiratory water loss in camels. Proceedings of Royal Society of London. Series B 211:291-303.

Schroter RC, Robertshaw D and Zine Filali R (1989). "Brain cooling and respiratory heat exchange in camels during rest and exercise." Respiration Physiology 78(1):95-105.

Smuts Malie MS and Bezuidenhout AJ (1987). Anatomy of The Dromedary. Oxford: Clarendon Press 1987:1-8, 106-109

Yang GC, Scherer PW and Mozell MM (2007). Modeling Inspiratory and Expiratory Steady-State Velocity Fields in the Sprague-Dawley Rat Nasal Cavity. Chemical Senses 32:215-223.

CAMEL PORTRAIT EXHIBIT AT *'FACES OF THE DESERT'* EXHIBITION OF AL NASSMA

Al Nassma Chocolate LLC (Al Nassma), the first company in the world to produce camel milk chocolate recently hosted the first ever camel portrait photo exhibition 'Faces of the Desert' in Umm Nahad, Dubai, together with Camelicious, the sole supplier of camel milk to Al Nassma.

The idea of this somewhat different photo exhibition was the brainchild of Ralf Baumgarten, a photographer with a passion for watches… and chocolate during an assignment with Al Nassma was touched by these beautiful animals.

Baumgarten and Woebers did not use artificial lighting during their sessions of sun-filled days in the desert, in order not to disturb the animals. Out of thousand of photographs, 40 portraits were chosen for the exhibition which was opened by Mr. Mutasher Al Badry of Camelicious. The opening drew a large crowd of people who came to see the portraits grace the entrance of the camel farm and the Al Nassma shop in Umm Nahad.

AL NASSMA CHOCOLATES NOW AVAILABLE AT DUBAI DUTY FREE AT DUBAI AIRPORT JUMEIRAH HOTELS & RESORTS

Al Nassma's range of exquisite camel milk chocolates are now available at Dubai Duty Free at terminal three and a host of Jumeirah Hotels & Resorts, in addition to its shop opposite the Camelicious camel farm. Residents and tourists alike will now be able to easily stock up on the sweet treat, the first ever camel milk chocolate in the world.

Al Nassma's range of 70 gram chocolate bars, are delicately flavoured with local spices, dates, macadamia nut and orange. Also available are whole milk, in addition to the favourite of chocoholics, the luxurious 70 percent cocoa. There is also a range of pralines delicately filled with pistachio, nougat and coffee cream, Email office@al-nassma.com or visit the website www.al-nassma.com for further details.